Comparative Study of the 3DCRT Dosimetric Response of Head Fricke Xylenol Gel Phantoms with and without Human Bone

Christianne C. Cavinato, Maíra T. Yoshizumi, Benedito H. Souza, Henrique Carrete, Jr., Kellen A. C. Daros, Regina B. Medeiros, Adelmo J. Giordani, Orlando Rodrigues, Jr., and Letícia L. Campos

***Abstract*—In this preliminary comparative study, the dosimetric response of two different head Fricke xylenol gel (FXG) phantoms, with and without human bone, prepared using 270 Bloom gelatin and irradiated with 6 MV photon beams using 3DCRT treatment, were evaluated employing magnetic resonance imaging (MRI) technique, in order to verify the difference of ionizing radiation absorption in head phantom due to the presence of human skull, to make a more reliable dosimetry. This study presents good results for 6 MV photons and 3DCRT treatment technique and no significative influence was observed due to the human skull presence. The obtained results encourage future studies using other complex treatment techniques, such as IMRT.**

***Index Terms*—Clinical photon beams, FXG phantom, magnetic resonance imaging, three-dimensional conformal radiotherapy.**

I. Introduction

Any failure in treatment planning for head tumors may result in intellectual impairment of the patient or drastically affect the functionality of other body parts [1]-[4]. That is why, increasingly, studies are carried out to maximize the effect of radiation on the tumor and minimize damage surrounding tissues. Complex radiation treatment techniques, such as three-dimensional conformal radiation therapy (3DCRT) and intensity modulated radiation therapy (IMRT), are used for this purpose [5], [6]. The greater the complexity of the treatment technique, the more accurate should be the quality control of treatment planning, and for this application, different dosimetric systems have been studied [7]-[9].

Manuscript received June 1, 2012. This work was supported by the CAPES, FAPESP, CNPq, IPEN, CNEN, MCT: Project INCT for Radiation Metrology in Medicine and MRA Indústria de Equipamentos Eletrônicos Ltda.

C. C. Cavinato, M. T. Yoshizumi, O. Rodrigues Jr. and L. L. Campos are of Gerência de Metrologia das Radiações, Instituto de Pesquisas Energéticas e Nucleares, Av. Prof. Lineu Prestes, 2242, Cidade Universitária, SP 05508-000 Brazil (corresponding author e-mail: ccavinato@ipen.br).

B. H. Souza, H. Carrete Jr., K. A. C. Daros and R. B. Medeiros are of Departamento de Diagnóstico por Imagens, Universidade Federal de São Paulo, Rua Napoleão de Barros, 800, SP 04024-002 Brazil.

A. J. Giordani is of Unidade de Radioterapia, Universidade de São Paulo, Rua Napoleão de Barros, 715, SP 04024-002 Brazil.

In this comparative study, the dosimetric response of two different head Fricke xylenol gel (FXG) phantoms, with and without human bone, prepared using 270 Bloom gelatin from porcine skin (made in Brazil) and irradiated with 6 MV photon beams using 3DCRT treatment technique, were evaluated employing magnetic resonance imaging (MRI) evaluation technique, in order to verify the difference of ionizing radiation absorption in head phantom due to the presence of human skull, to make a more reliable dosimetry.

II. Materials and Methods

A. FXG Solutions Preparation

The FXG solutions were prepared as in [10], at High Doses Laboratory (LDA) of Nuclear and Energy Research Institute (IPEN) using 5% by weight 270 Bloom gelatin from porcine skin, ultra-pure water, 50 mM sulphuric acid (H_2SO_4), 1 mM sodium chloride (NaCl), 1 mM ferrous ammonium sulphate hexahydrate [$Fe(NH_4)_2(SO_4)_2.6H_2O$] and 0.1 mM ferric ions indicator xylenol orange ($C_{31}H_{28}N_2Na_4O_{13}S$).

B. FXG Solutions Conditioning

The FXG solution was conditioned in polymethyl methacrylate (PMMA) cuvettes (10 x 10 x 45 mm^3) (Fig. 1) to obtain calibration curves. Sets of three samples each were prepared and packed with polyvinyl chloride (PVC) film to prevent evaporation of the water contained in the FXG solution and to ensure the reproducibility of the dosimetric response of the three FXG samples.

The dosimetric solution was also conditioned in a spherical glass balloon of 2000 mL (156 mm internal diameter and 2 mm wall thickness) (Fig. 2) and a PMMA rectangular box with separate lid (17 x 20 x 16 cm^3 and 3 mm wall thickness), containing a adult human skull (Fig. 3), in order to conform two different head FXG phantoms, without and with human bone.

The PMMA cuvettes and head phantoms were maintained under low temperature ((4 ± 1) ºC) and light protected during about 12 hours after preparation.

C. *Treatment Planning*

To perform the 3DCRT treatment planning, computed tomography (CT) scans were obtained from head phantoms without and with human bone filled with water, instead of Fricke xylenol gel solution, using a Philips® Brilliance CT 64-channel scanner of the Diagnostic Image Department of Sao Paulo Hospital (HSP) of Federal University of Sao Paulo (UNIFESP).

The Eclipse® External Beam Planning system version 7.3.10 was used for axial CT images slices processing. These CT images corresponding to the head phantoms without and with human bone are presented in Fig. 4.

Fig. 1. PMMA cuvettes set filled with FXG solution.

Fig. 2. Spherical glass balloon filled with FXG solution: the head FXG phantom without human bone.

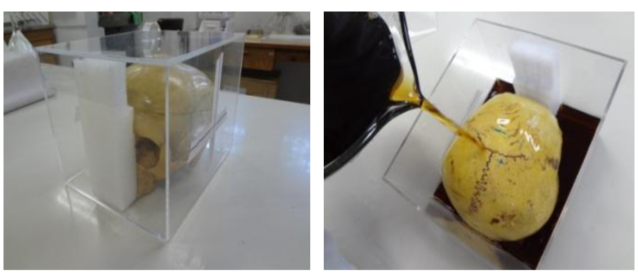

Fig. 3. PMMA rectangular box containing a adult human skull filled with FXG solution: head FXG phantom with human bone.

D. *Irradiation*

The cuvettes and phantoms were stored in a Styrofoam box (with lip) containing ice reusable in order to keep them under low temperature and light protected to be transported to the irradiation site. They were maintained at room temperature and light protected for 30 minutes before irradiation.

The irradiations were carried out in the Radiotherapy Service of HSP/UNIFESP.

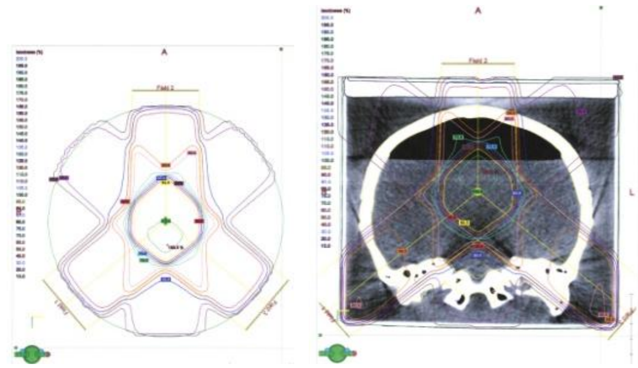

a b

Fig. 4. Three-dimensional treatment planning for head FXG phantoms without (a) and with (b) human bone.

PMMA Cuvettes

To obtain the calibration curves, the PMMA cuvettes sets were positioned at source-surface distance (SSD) of 80 cm in a PMMA phantom (30 x 30 cm^2 plates 1.5 cm thick), 40 x 40 cm^2 radiation field size and irradiated with different photon doses ranging from 2 to 30 Gy and dose rate of 74.98 $cGy.min^{-1}$, using a GENERAL ELECTRIC COMPANY® Alcyon II ^{60}Co gamma radiation therapy machine. All cuvettes sets were positioned together in the PMMA phantom and each set was removed when the radiation exposure time needed to obtain the desired absorbed dose was completed.

The ^{60}Co gamma radiation was applied to the cuvettes filled with FXG solution, considering: the homogeneity and precision of absorbed dose delivery of ^{60}Co gamma sources and that the effective photon energy of 6 MV photon beams is approximately 2 MeV.

Head FXG Phantoms

The head phantoms were irradiated with 6 MV clinical photon beams, absorbed dose of 20 Gy, dose rate of 300 $cGy.min^{-1}$, SSD of 91.9 cm, using multiple static radiation fields of a VARIAN® Clinac 600C linear accelerator. The other irradiation parameters and experimental set-ups for phantoms irradiations are presented in Table 1 and Fig. 5, respectively.

TABLE I
IRRADIATION PARAMETERS FOR THE FXG PHANTOMS

	Radiation Fields		
	1	2	3
Gantry Position (º)	230.0	0.0	130.0
Treatment Couch Position (º)	0.0	0.0	0.0
X1, X2, Y1, Y2 Fields Size (cm)	+ 2.5	+ 2.5	+ 2.5
SSD (cm)	91.9	91.9	91.0
Monitor Unit (MU)	853	854	854

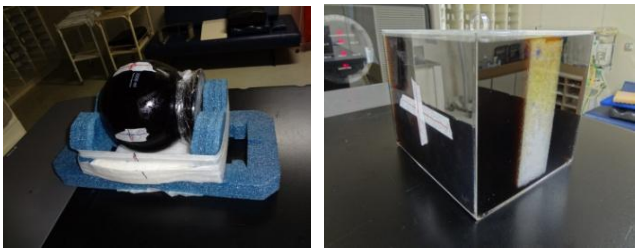

a b

Fig. 5. Experimental set-ups for irradiation of the head FXG phantoms without (a) and with (b) human bone.

The evaluation techniques used in this study were the optical absorption (OA) spectrophotometry and magnetic resonance imaging (MRI).

The OA measures were performed immediately after FXG solution preparation and approximately 30 minutes after irradiation, using a SHIMADZU® UV2101-PC spectrophotometer (LDA/IPEN) and wavelength range of 190 to 900 nm. The absorbance values presented correspond to dosimetric wavelength of 585 nm [11]. This evaluation technique was used only as reference system.

The PMMA cuvettes and head phantoms MRI images were acquired approximately 30 minutes after irradiation using a SIEMENS® MAGNETOM® Sonata Maestro Class 1.5 T MRI scanner of the Resonance Magnetic Service at Diagnostic Image Department of HSP/UNIFESP, on cranium protocol-T1. The MRI images acquisition parameters are presented in Table 2. To MRI images processing, the softwares syngo fastView® version VX57F24 and ImageJ® version 1.42q were used.

Both the OA and MRI calibration curves, each presented value corresponds to the average of the measurement of three samples and the error bars the standard deviation of the mean. The background values corresponding to the optical and magnetic measurements of non-irradiated Fricke gel samples were subtracted from all values presented.

TABLE II
MRI IMAGES ACQUISITION PARAMETERS

Parameters Description	Values
Image Orientation	Coronal, sagittal and axial
Field of View (FOV) (mm)	256
Slice Thickness (THK) (mm)	3.0
Voxel (mm)	1.0x1.0x1.0
Gap (mm)	3.0
Time of Repetition (TR) (ms)	2000
Time of Echo (TE) (ms)	3.42
Flip Angle (º)	15
Matrix Size (MS) (pixels)	256x256
Number of Signals Averaged (NSA)	1
Slices Number	41
Coil	Head
Channels	8

The Python scripts were used for post-processing the following tasks: identifying of the information in DICOM files and calibration curve fitting. The images were generated using custom software written in MATLAB. Isodose curves were calculated as a percentage of the dose to the central axis slices of MR images.

III. RESULTS AND DISCUSSION

A. Dose-Response Curves

The optical dose-response curve of the Fricke xylenol gel solution irradiated with ^{60}Co gamma radiation, absorbed dose range from 2 to 30 Gy, is presented in Fig. 6.

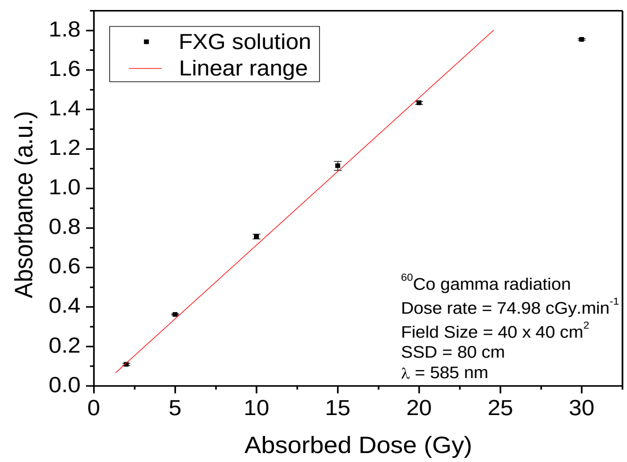

Fig. 6. Optical dose-response curve of the FXG solution irradiated (^{60}Co gamma radiation).

The coronal PMMA cuvettes MRI image slice of the FXG solution non-irradiated and irradiated with ^{60}Co gamma radiation (2 to 30 Gy), is presented in Fig. 7.

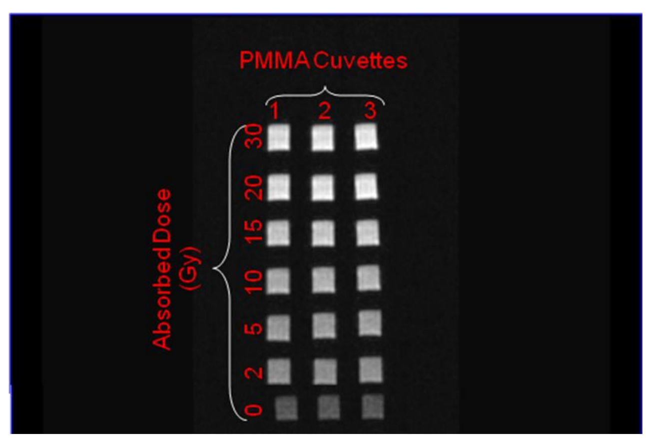

Fig. 7. Coronal PMMA cuvettes MRI image slice of the FXG solution non-irradiated and irradiated with ^{60}Co gamma radiation.

The MRI signal intensity curve in function of absorbed dose, obtained from PMMA cuvettes MRI images presented in Fig. 7, is presented in Fig. 8.

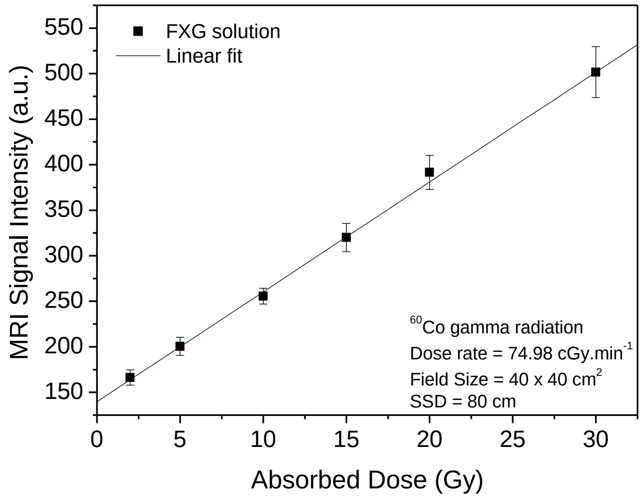

Fig. 8. MRI signal intensity curve in function of absorbed dose.

The calibration curves presented linear behavior in the clinical interest dose range (2 to 20 Gy) for both evaluation techniques (OA and MRI), tending to optical saturation to doses ≥ 20 Gy.

B. MRI Slices Images: FXG Phantoms

The coronal, sagittal and axial MRI image slices of the head FXG phantom without human bone, irradiated with 6 MV photons and 20 Gy, are presented in Fig. 9, 10 and 11, respectively.

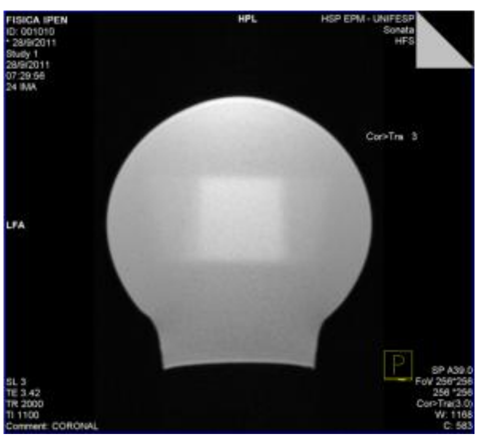

Fig. 9. Coronal MRI image slice of the head FXG phantom without human bone (6 MV photons and 20 Gy).

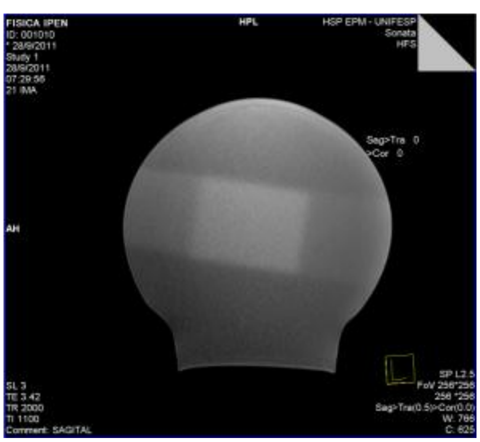

Fig. 10. Sagittal MRI image slice of the head FXG phantom without human bone (6 MV photons and 20 Gy).

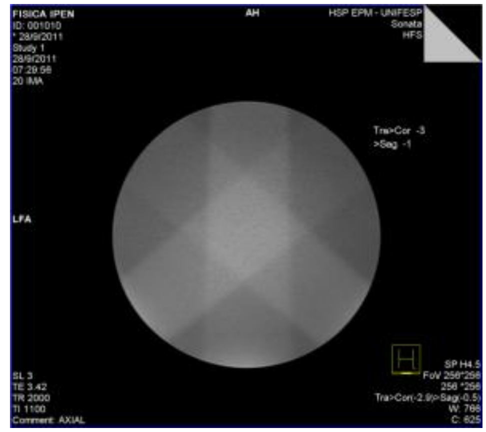

Fig. 11. Axial MRI image slice of the head FXG phantom without human bone (6 MV photons and 20 Gy).

The coronal, sagittal and axial MRI image slices of the head FXG phantom with human bone, irradiated with 6 MV photons and 20 Gy, are presented in Fig. 12, 13 e 14, respectively.

Fig. 12. Coronal MRI image slice of the head FXG phantom with human bone (6 MV photons and 20 Gy).

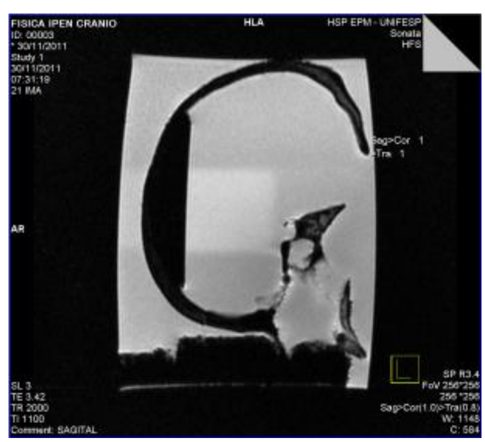

Fig. 13. Sagittal MRI image slice of the head FXG phantom with human bone (6 MV photons and 20 Gy).

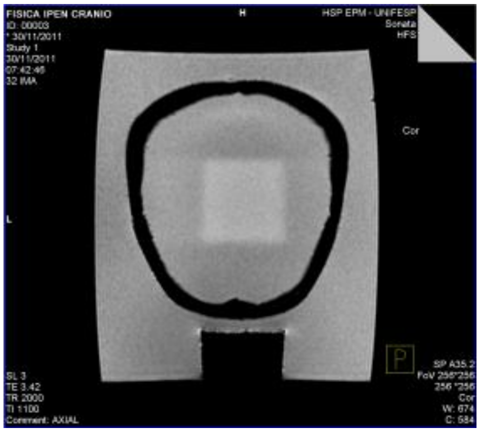

Fig. 14. Axial MRI image slice of the head FXG phantom with human bone (6 MV photons and 20 Gy).

The irradiated target volume can be defined in the MRI images slices at coronal, sagittal and axial orientations. In the axial and coronal MRI image slices (Figs. 11 and 12) can also be seen the imput and the overlap of multiple radiation fields.

C. Isodose Curves

The isodose curves determined for coronal, sagittal and axial MRI image slices of the head FXG phantom without human bone, irradiated with 6 MV photons and 20 Gy, are presented in Fig. 15, 16 e 17, respectively.

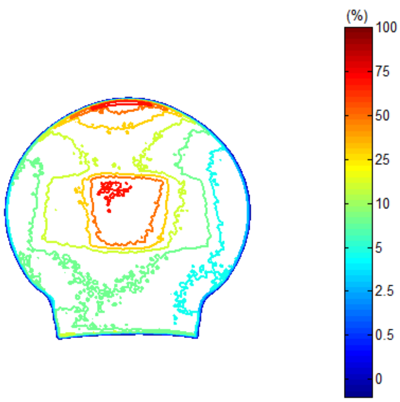

Fig. 15. Isodose curves determined for coronal MRI image slice of the head FXG phantom without human bone (6 MV photons and 20 Gy).

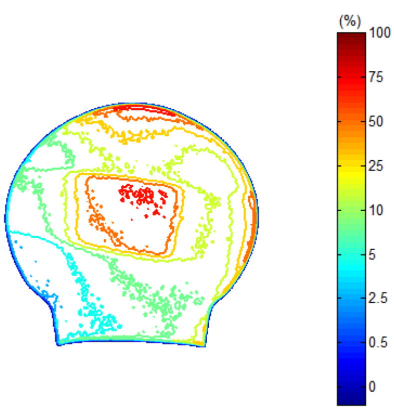

Fig. 16. Isodose curves determined for sagittal MRI image slice of the head FXG phantom without human bone (6 MV photons and 20 Gy).

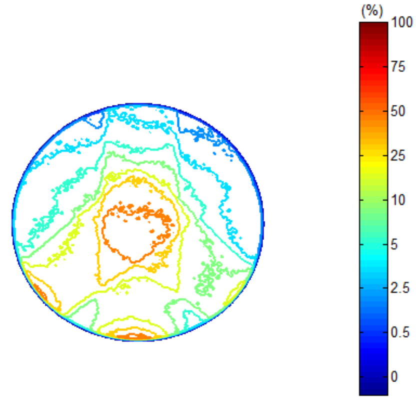

Fig. 17. Isodose curves determined for axial MRI image slice of the head FXG phantom without human bone (6 MV photons and 20 Gy).

The isodose curves determined for coronal, sagittal and axial MRI image slices of the head FXG phantom with human bone, irradiated with 6 MV photons and 20 Gy, are presented in Fig. 18, 19 and 20, respectively.

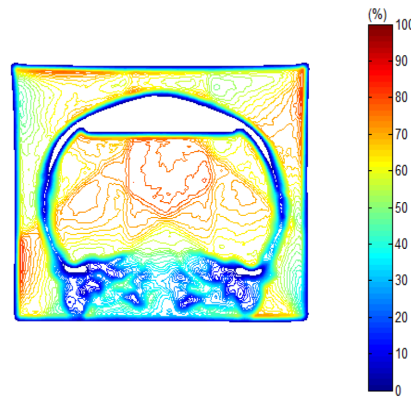

Fig. 18. Isodose curves determined for coronal MRI image slice of the head FXG phantom with human bone (6 MV photons and 20 Gy).

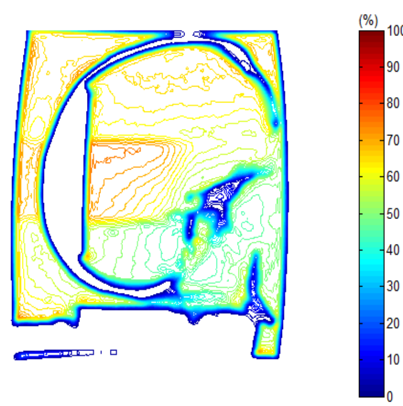

Fig. 19. Isodose curves determined for sagittal MRI image slice of the head FXG phantom with human bone (6 MV photons and 20 Gy).

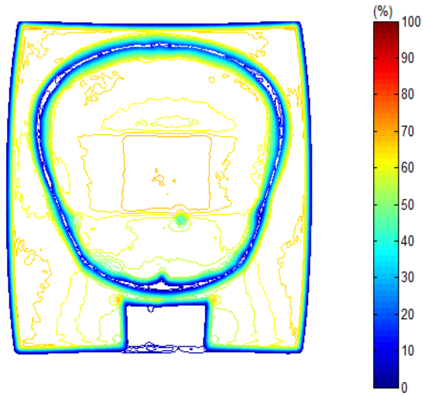

Fig. 20. Isodose curves determined for axial MRI image slice of the head FXG phantom with human bone (6 MV photons and 20 Gy).

In both head FXG phantoms (with and without human bone) the irradiated target volume received the maximum percentage of the dose as expected. The high percentage of the dose in imput of multiple radiation fields can also be observed.

IV. Conclusion

The preliminary comparative study of the different head FXG phantoms with and without human bone presents good results for 6 MV photons and 3DCRT treatment technique. No significative influence was observed due to the human skull presence and the obtained results encourage future studies using other complex treatment techniques, such as IMRT.

Acknowledgment

The authors thanks to the staffs of the Radiotherapy Service and Resonance Magnetic Service of the Diagnostic Image Department of the HSP/UNIFESP to allow the FXG irradiations and MRI evaluations, respectively.

References

[1] L. S. Constine, P. D. Woolf, D. Cann, G. Mick, K. McCormick, R. F. Raubertas, and P. Rubin, "Hypothalamic-Pituitary Dysfunction after Radiation for Brain Tumors," *N. Engl. J. Med.*, vol. 328, pp. 87-94, Jan. 1993.

[2] G. Di Chiro, E. Oldfield, D. C. Wright, D. De Michele, D. A. Katz, N. J. Patronas, J. L. Doppman, S. M. Larson, M. Ito, and C. V. Kufta, "Cerebral necrosis after radiotherapy and/or intraarterial chemotherapy for brain tumors: PET and neuropathologic studies," *American Journal of Roentgenology*, vol. 150, no. 1, pp. 189-197, Jan. 1988.

[3] R. K. Mulhern, J. J. Crisco, and L. E. Kun, "Neuropsychological sequelae of childhood brain tumors: A review," *Journal of Clinical Child Psycholog*, vol. 12, no. 1, pp. 66-73, 1983.

[4] R. S. Scheibel, C. A. Meyers, and V. A. Levin, "Cognitive dysfunction following surgery for intracerebral glioma: influence of histopathology, lesion location, and treatment," *Journal of Neuro-Oncology*, vol. 30, no. 1, pp. 61-69, 1996.

[5] A. T. C. Chan, P. M. L. Teo, and P. J. Johnson, "Nasopharyngeal carcinoma," *Annals of Oncology*, vol. 13, pp. 1007-1015, 2002

[6] R. M 3rd., "Reducing the toxicity associated with the use of radiotherapy in men with localized prostate cancer," *Urol. Clin. North Am.*, vol. 31, no. 2, pp. 353-366, May 2004.

[7] L. J. Schreiner, "Review of Fricke gel dosimeters," *Journal of Physics: Conference Series*, vol. 3, pp. 9-21, 2004.

[8] C. Wuu, and Y. Xu, "Three-dimensional dose verification for intensity modulated radiation therapy using optical CT based polymer gel dosimetry," *Medical Physics*, vol. 33, no. 5, pp. 1412-1419, 2006.

[9] W. C. Chu, "Radiation dosimetry using Fricke-infused gels and magnetic resonance imaging," *Proceedings of the National Science Council, Republic of China – Part B*, vol. 25, no. 1, pp. 1-11, 2001.

[10] L. E. Olsson, S. Petersson, L. Ahlgren, and S. Mattsson, "Ferrous sulphate gels for determination of absorbed dose distributions using MRI technique: basic studies," *Physics in Medicine and Biology*, vol. 34, no. 1, pp. 43-52, 1989.

[11] M. A. Bero, W. B. Gilboy, and P. M. Glover, "Radiochromic gel dosemeter for three-dimensional dosimetry," *Radiation Physics and Chemistry*, vol. 61, pp. 433-435, 2001.